Biocatalysis

International Edition: DOI: 10.1002/anie.201606722
German Edition: DOI: 10.1002/ange.201606722

Directed Evolution of a Fluorinase for Improved Fluorination Efficiency with a Non-native Substrate

Huihua Sun[+], Wan Lin Yeo[+], Yee Hwee Lim[+], Xinying Chew, Derek John Smith, Bo Xue, Kok Ping Chan, Robert C. Robinson, Edward G. Robins, Huimin Zhao, and Ee Lui Ang**

Abstract: *Fluorinases offer an environmentally friendly alternative for selective fluorination under mild conditions. However, their diversity is limited in nature and they have yet to be engineered through directed evolution. Herein, we report the directed evolution of the fluorinase FlA1 for improved conversion of the non-native substrate 5′-chloro-5′-deoxyadenosine (5′-ClDA) into 5′-fluoro-5′-deoxyadenosine (5′-FDA). The evolved variants, fah2081 (A279Y) and fah2114 (F213Y, A279L), were successfully applied in the radiosynthesis of 5′-[^{18}F]FDA, with overall radiochemical conversion (RCC) more than 3-fold higher than wild-type FlA1. Kinetic studies of the two-step reaction revealed that the variants show a significantly improved k_{cat} value in the conversion of 5′-ClDA into S-adenosyl-L-methionine (SAM) but a reduced k_{cat} value in the conversion of SAM into 5′-FDA.*

Organofluorine compounds play important roles in pharmaceuticals,[1] agrochemicals,[2] materials,[3] and positron emission tomography (PET)[4] imaging. Many advances have been made in C–F bond formation,[5] while selective fluorination under mild conditions remains challenging. The discovery and characterization of four naturally occurring fluorinase enzymes (FlA,[6] FlA1,[7] FlA3[7] and NobA[7–8]) offers an attractive prospect for using biocatalysts to produce fluorinated compounds.[9] These fluorinases convert *S*-adenosyl-L-methionine (SAM) and fluoride ions into 5′-fluoro-5′-deoxyadenosine (5′-FDA) and L-methionine (L-Met) through a nucleophilic substitution (S_N2) mechanism.[10] Pioneering work by O'Hagan's group has demonstrated the application of the fluorinase FlA in the radiosynthesis of 5′-[^{18}F]FDA,[11] as well as the coupling of FlA with additional enzymes to produce a range of ^{18}F-labeled nucleosides[12] and a ^{18}F-labeled sugar[11b,13] for PET applications.[14]

To explore the substrate promiscuity for broader applications, FlA has been reported to accept 5′-chloro-5′-deoxyadenosine (5′-ClDA),[15] 2′-deoxyadenosine substrates,[16] L-Met analogues,[17] a methylaza analogue of SAM,[18] 5′-chlorodeoxy-2-ethynyladenosine (ClDEA),[19] and even highly complex di- and tetra-cyclic peptide conjugates[20] of ClDEA. It is noteworthy that the catalytic efficiency of wild-type fluorinases with non-native substrates is often reduced.[17–19] Powerful enzyme engineering approaches such as directed evolution[21] and rational protein design[22] can potentially restore the impaired activity. Thomsen et al. identified a FlA mutant with increased activity for the ethyl analogue of L-Met through a series of rationally designed point mutations.[17] However, directed evolution has yet to be employed to engineer fluorinases. Herein, we report directed evolution of the fluorinase FlA1 to improve the fluorination efficiency for the non-native substrate 5′-ClDA.

5′-ClDA is an attractive substrate that could be fluorinated in the presence of L-Met (Scheme 1).[15] It can be

[*] Dr. H. Sun,[+] W. L. Yeo,[+] Prof. Dr. H. Zhao, Dr. E. L. Ang
Metabolic Engineering Research Laboratory (MERL)
Science and Engineering Institutes
Agency for Science, Technology, and Research (A*STAR)
31 Biopolis Way, Nanos #01-01, Singapore 138669 (Singapore)
E-mail: angel@merl.a-star.edu.sg
Prof. Dr. H. Zhao
215 Roger Adams Laboratory, Box C3
University of Illinois at Urbana-Champaign
600 South Mathews Avenue, Urbana, IL 61801 (USA)
E-mail: zhao5@illinois.edu
Dr. Y. H. Lim,[+] X. Chew, Dr. K. P. Chan
Institute of Chemical and Engineering Sciences (ICES), A*STAR
8 Biomedical Grove, Neuros #07-01/02/03, Singapore 138665 (Singapore)
Dr. D. J. Smith
Bioinformatics Institute, A*STAR
30 Biopolis Street, Matrix #07-01, Singapore 138671 (Singapore)
and
Biotransformation Innovation Platform
61 Biopolis Drive, Proteos #04–14, Singapore 138673 (Singapore)
Dr. B. Xue, Prof. R. C. Robinson
Institute of Molecular and Cell Biology (IMCB), A*STAR
61 Biopolis Drive, Proteos #03–15, Singapore 138673 (Singapore)
Prof. R. C. Robinson
Department of Biochemistry, Yong Loo Lin School of Medicine
National University of Singapore, Singapore 117597 (Singapore)
and
NTU Institute of Structural Biology
Nanyang Technological University (NTU)
59 Nanyang Drive, Singapore 636921 (Singapore)
and
School of Biological Sciences, NTU
60 Nanyang Drive, Singapore 637551 (Singapore)
and
Lee Kong Chian School of Medicine
50 Nanyang Avenue, Singapore 639798 (Singapore)
Dr. E. G. Robins
Singapore Bioimaging Consortium (SBIC), A*STAR
11 Biopolis way, #02-02, Singapore 138667 (Singapore)
[+] These authors contributed equally to this work.
Supporting information and the ORCID identification number(s) for the author(s) of this article can be found under http://dx.doi.org/10.1002/anie.201606722.

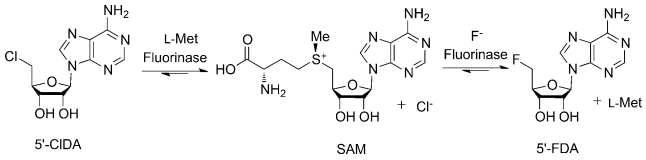

Scheme 1. The two-step conversion of 5′-ClDA into 5′-FDA by fluorinases.

readily synthesized and has good chemical stability. FlA1 from *Streptomyces* sp. MA37 was adopted as the parent enzyme for directed evolution since FlA1 has been reported to be the most efficient fluorinase for SAM[7] and we have found that FlA1 shows relatively higher activity with 5′-ClDA among the four fluorinases (Figure S1 in the Supporting Information). Saturation mutagenesis libraries were constructed by targeting 23 residues within 5 Å from SAM in a FlA1 homology model based on the structure of FlA (PDB ID: 1RQP). The gene encoding nucleoside phosphorylase (PNP) in *Escherichia coli* BL21 (DE3) was knocked out in order to prevent 5′-FDA degradation by PNP in the cell lysate. Then, the NNK libraries were cloned and expressed in the BL21 (DE3) ΔPNP strain. A total of 1932 (23 × 84) clones were screened in high-throughput assays.

The screening identified fah2047 (A279L), fah2081 (A279Y) and fah2019 (F213Y) as the top variants with improved 5′-FDA yields (Table S1 in the Supporting Information). The mutation F213Y was introduced to fah2047 to give fah2114 (F213Y, A279L). FlA1 (FlA1 refers to wild-type FlA1) and the variants (fah2047, fah2081, and fah2114) were purified for validation through in vitro reactions. Since purified fah2114 was found to be bound with SAM, which cannot be removed (Figure S2), control reactions were run without 5′-ClDA and L-Met to exclude the 5′-FDA produced from endogenous SAM. At 37 °C, all of the purified variants achieved higher 5′-FDA yields than FlA1 at both 4 h and 24 h (Figure S3).

To optimize the reaction conditions, we increased the reaction temperature and found that the fluorinases were more active at 42 °C (Figure S4). Enzyme concentrations and substrate concentrations were also optimized for higher 5′-FDA yields (data not shown). Under the optimized conditions, we compared the reactions with either L-Met or L-selenomethionine (L-SeMet; Figure 1). In the presence of L-Met, fah2081 and fah2114 gave 2.4- to 2.7-fold higher yields than FlA1 at 90 min (Table S2). The use of L-SeMet increased the yield by around 2-fold for all of the fluorinases.

Subsequently, the evolved fluorinases fah2081 and fah2114 were used for the radiosynthesis of 5′-[^{18}F]FDA. The reaction conditions were optimized to achieve high radiochemical conversion (RCC). We found that the RCC is dependent on fluorinase concentration despite [^{18}F]fluoride being the limiting reagent (Figure S5). Moreover, the highest conversion was observed when the concentration of 5′-ClDA was approximately 4-fold that of fluorinase concentration (Figure S6). At 42 °C, the overall RCC for fah2081 is 3.4-fold higher than that for FlA1 (Table 1). Since both fah2114 and FlA1 are stable at 47 °C and higher temperatures may further boost the RCC, we compared fah2114 with FlA1 at 47 °C. The

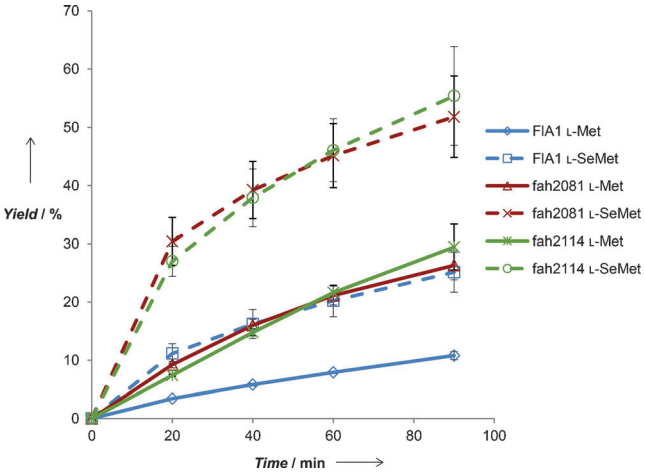

Figure 1. Comparison of the activity of FlA1 and the variants with 5′-ClDA at 42 °C. Optimized conditions: 0.2 mM 5′-ClDA, 0.1 mM L-Met/L-SeMet, 100 mM NaF, and 150 μM fluorinase. Yield = (concentration of 5′-FDA generated/ concentration of the substrate 5′-ClDA) × 100 %.

Table 1: Comparison of the radiosynthesis efficiency of FlA1 and the variants.

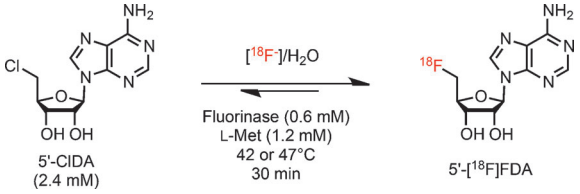

Fluorinase	*T* [°C]	RCC (analytical) [%]	RCC[a] (overall) [%]
FlA1	42	8 ± 1	7 ± 1
FlA1	47	11 ± 2	8 ± 2
fah2081 (A279Y)	42	32 ± 3	24 ± 2
fah2114 (F213Y, A279L)	47	46 ± 2	34 ± 3

[a] Overall RCC = % radioactivity in supernatant × % RCC based on radioHPLC. Typical % radioactivity in supernatant is in the range 73–80 %.

overall RCC for fah2114 is 4.3-fold higher than that for FlA1 at 47 °C. Thus, both evolved variants are at least 3-fold more efficient than FlA1 in the radiosynthesis of 5′-[^{18}F]FDA.

To understand how the variants improved the conversion of 5′-ClDA into 5′-FDA, kinetic studies of the two-step reaction (Scheme 1) were carried out for FlA1, fah2081, and fah2114 (Tables 2 and 3 and Figure S7, S8). In the first step (conversion of 5′-ClDA into SAM; Table 2), fah2081 and fah2114 show faster turnover, with k_{cat} values 4- and 29-fold larger, respectively, than that of FlA1. On the other hand, fah2081 and fah2114 are slower in the second step (conversion of SAM into 5′-FDA; Table 3), with k_{cat} values 2- and 9-fold smaller, respectively, than that of FlA1. These kinetics data reveal that only the first step of the reaction is significantly accelerated by the directed evolution. The higher k_{cat} value in the first step is able to compensate for the slowing of the second step, thereby resulting in an overall improved conversion of 5′-ClDA into 5′-FDA.

Table 2: Comparative kinetics data for FlA1 and the variants for the conversion of 5′-ClDA into SAM.[a]

Fluorinase	V_{max} [μM min^{-1}]	5′-ClDA K_m [μM]	k_{cat} [min^{-1}]	[k_{cat}/K_m] [mM^{-1} min^{-1}]
FlA1	0.67 ± 0.04	8.36 ± 0.82	0.13	16.08
fah2081	2.66 ± 0.22	59.26 ± 4.44	0.53	8.96
fah2114	19.28 ± 0.44	9.45 ± 2.22	3.86	407.91

[a] Assays contain 20 mM L-Met and various concentrations of 5′-ClDA.

Table 3: Comparative kinetic data of FlA1 and the variants for the conversion of SAM into 5′-FDA.[a]

Fluorinase	V_{max} [μM min^{-1}]	SAM K_m [μM]	k_{cat} [min^{-1}]	[k_{cat}/K_m] [mM^{-1} min^{-1}]
FlA1	4.47 ± 0.21	34.55 ± 1.94	0.22	6.47
fah2081	2.12 ± 0.09	22.22 ± 1.72	0.11	4.78
fah2114	0.47 ± 0.02	9.24 ± 0.65	0.02	2.57

[a] Assays contain 200 mM NaF and various concentrations of SAM.

The structure of FlA1 has been reported,[7a] but the data were not initially publicly accessible.[7b] We crystallized the wild-type FlA1 in space group $P2_13$ and solved the structure to a resolution of 1.95 Å (Figure 2; also see Figure S9 and Table S3). FlA1 is composed of a dimer of trimers, similar to that observed in the homologous FlA structures.[10b] This hexameric assembly was confirmed by size-exclusion chromatography (Figure S10). Adenosine and L-Met are bound at the interface between two neighboring monomers. HPLC analysis shows a much higher amount of adenosine bound to purified FlA1 than the variants (Figure S2).

To gain structural insight into the mutations, homology models of trimeric fah2081 and fah2114 complexed to SAM

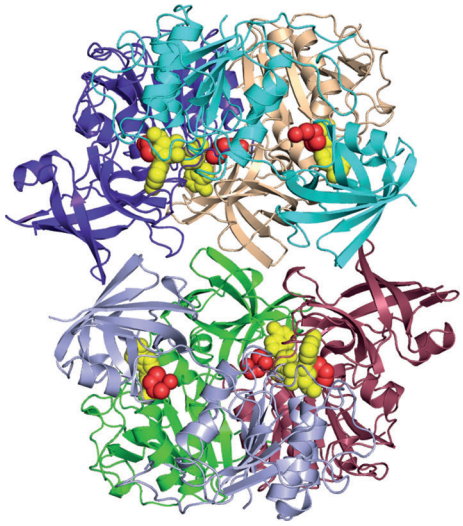

Figure 2. The hexameric structure of FlA1 (PDB ID: 5B6I) shown as a ribbon diagram. Trimer A is formed by monomer A (purple), monomer B (cyan), and monomer C (beige). Trimer B is formed by monomer D (green), monomer E (pale purple), and monomer F (dark red). Adenosine (yellow) and L-Met (red) are shown as spheres.

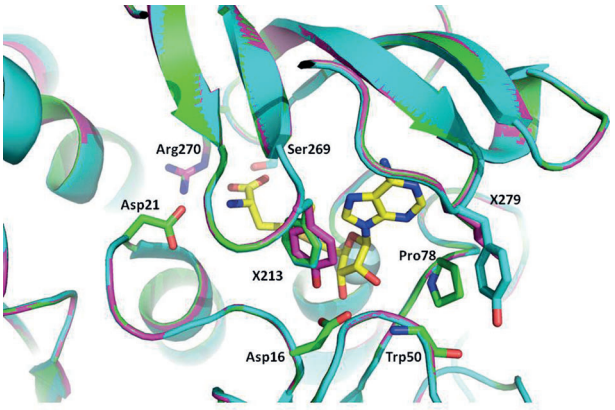

Figure 3. Models of FlA1 mutants. A close-up of the SAM-binding sites of FlA1 (green), fah2081 (cyan), and fah2114 (magenta), showing the mutated positions at 213 and 279 as stick models. SAM is also shown as a stick model (C yellow; O red; N blue).

(Figure 3) were generated using our FlA1 crystal structure as a template. Mutation at position 279 to bulkier residues may restrict the movement of the 277–281 loop located above the adenine ring, thereby leading to a tighter binding of the adenine. Both mutations are close to the sidechain of Pro78, and may participate in favorable hydrophobic contacts. Leu279 of fah2114 is also within van der Waals contact of an aromatic carbon in the adenine ring, thereby improving the favorable hydrophobic environment. In addition, Tyr213 of fah2114 is involved in polar interaction with Asp16, which would act as a clamp between the protein monomers across the ribose ring. Both of these monomers are also involved in binding of the methionine moiety in SAM through 1) Ser269 and Arg270 on the monomer harboring Tyr213, and 2) Asp21 on the adjacent monomer harboring Asp16. Consequently, tightening of the dimer interface through favorable interactions along the binding site leads to further improved binding of SAM.

The structural implications of stronger binding of SAM explain the higher affinities of fah2081 and fah2114 for SAM (lower SAM K_m) compared to FlA1 (Table 2). The very high affinity of fah2114 for SAM is also consistent with the observation that SAM is copurified with fah2114 (Figure S2). Prior occupation of the pocket with SAM could impede the binding of solvated F^- to the enzyme (since SAM is a "competitive" inhibitor[10c] of F^- binding). The binding of solvated F^- to an unoccupied pocket is the initial step of fluorination, which is followed by desolvation of F^- driven by SAM binding and then the S_N2 attack.[10c] Hence, the stronger binding of SAM may cause the decreased k_{cat} observed for fah2081 and fah2114 in the conversion of SAM into 5′-FDA.

In conclusion, we have engineered the fluorinase FlA1 through directed evolution and identified variants with improved activity for the non-native substrate 5′-ClDA. The evolved fluorinases, fah2081 and fah2114, were used to produce 5′-[^{18}F]FDA, with overall RCC values 3.4- and 4.3-fold higher, respectively, than FlA1. Kinetics studies indicated that the variants improve the activity with 5′-ClDA mainly through improvement of the k_{cat} value in the first step of the reaction (conversion of 5′-ClDA into SAM). This work

represents the first demonstration that the catalytic efficiency of a fluorinase on a non-native substrate can be improved through directed evolution. Directed evolution is expected to be widely employed to improve the catalytic efficiency of fluorinases with a broad range of substrates for industrial applications in the future. Endeavors in directed evolution will hopefully lead to a collection of beneficial mutations for specific substrates, which could offer deeper insight into the structure–function relationships and in turn facilitate rational-design-based fluorinase engineering.

Acknowledgements

This work was funded by the GlaxoSmithKline—Singapore Economic Development Board partnership for green and sustainable manufacturing, A*STAR ICES, and A*STAR IMCB. We thank members of MERL for their comments and Saei Weng Chia from SBIC for his assistance during the radiolabeling work.

Keywords: biocatalysis · directed evolution · fluorinases · halogenation · radiosynthesis

[1] a) K. Muller, C. Faeh, F. Diederich, *Science* **2007**, *317*, 1881 – 1886; b) S. Purser, P. R. Moore, S. Swallow, V. Gouverneur, *Chem. Soc. Rev.* **2008**, *37*, 320 – 330; c) S. Swallow, *Prog. Med. Chem.* **2015**, *54*, 65 – 133; d) E. P. Gillis, K. J. Eastman, M. D. Hill, D. J. Donnelly, N. A. Meanwell, *J. Med. Chem.* **2015**, *58*, 8315 – 8359.

[2] P. Jeschke, *ChemBioChem* **2004**, *5*, 571 – 589.

[3] D. W. Grainger, C. W. Stewart in *Fluorinated Surfaces, Coatings, and Films*, *Vol. 787*, American Chemical Society, Washington, **2001**, pp. 1 – 14.

[4] a) S. M. Ametamey, M. Honer, P. A. Schubiger, *Chem. Rev.* **2008**, *108*, 1501 – 1516; b) M. M. Alauddin, *Am. J. Nucl. Med. Mol. Imaging* **2012**, *2*, 55 – 76; c) O. Jacobson, D. O. Kiesewetter, X. Chen, *Bioconjugate Chem.* **2015**, *26*, 1 – 18.

[5] a) T. Furuya, A. S. Kamlet, T. Ritter, *Nature* **2011**, *473*, 470 – 477; b) C. D. Murphy, G. Sandford, *Expert Opin. Drug Metab. Toxicol.* **2015**, *11*, 589 – 599; c) M. G. Campbell, T. Ritter, *Chem. Rev.* **2015**, *115*, 612 – 633; d) J.-W. Lee, M. T. Oliveira, H. B. Jang, S. Lee, D. Y. Chi, D. W. Kim, C. E. Song, *Chem. Soc. Rev.* **2016**, *45*, 4638 – 4650.

[6] a) D. O'Hagan, C. Schaffrath, S. L. Cobb, J. T. G. Hamilton, C. D. Murphy, *Nature* **2002**, *416*, 279-279; b) C. Schaffrath, H. Deng, D. O'Hagan, *FEBS Lett.* **2003**, *547*, 111 – 114.

[7] a) H. Deng, L. Ma, N. Bandaranayaka, Z. Qin, G. Mann, K. Kyeremeh, Y. Yu, T. Shepherd, J. H. Naismith, D. O'Hagan, *ChemBioChem* **2014**, *15*, 364 – 368; b) The crystal structure of FlA1 was made public in the Protein Data Bank on 2 August 2016 (PDB ID: 5LMZ), after the submission of this communication.

[8] Y. Wang, Z. Deng, X. Qu, *F1000Res.* **2014**, *3*, 61.

[9] D. O'Hagan, H. Deng, *Chem. Rev.* **2015**, *115*, 634 – 649.

[10] a) C. D. Cadicamo, J. Courtieu, H. Deng, A. Meddour, D. O'Hagan, *ChemBioChem* **2004**, *5*, 685 – 690; b) C. J. Dong, F. L. Huang, H. Deng, C. Schaffrath, J. B. Spencer, D. O'Hagan, J. H. Naismith, *Nature* **2004**, *427*, 561 – 565; c) X. Zhu, D. A. Robinson, A. R. McEwan, D. O'Hagan, J. H. Naismith, *J. Am. Chem. Soc.* **2007**, *129*, 14597 – 14604.

[11] a) L. Martarello, C. Schaffrath, H. Deng, A. D. Gee, A. Lockhart, D. O'Hagan, *J. Labelled Compd. Radiopharm.* **2003**, *46*, 1181 – 1189; b) H. Deng, S. L. Cobb, A. D. Gee, A. Lockhart, L. Martarello, R. P. McGlinchey, D. O'Hagan, M. Onega, *Chem. Commun.* **2006**, 652 – 654.

[12] M. Winkler, J. Domarkas, L. F. Schweiger, D. O'Hagan, *Angew. Chem. Int. Ed.* **2008**, *47*, 10141 – 10143; *Angew. Chem.* **2008**, *120*, 10295 – 10297.

[13] M. Onega, J. Domarkas, H. Deng, L. F. Schweiger, T. A. Smith, A. E. Welch, C. Plisson, A. D. Gee, D. O'Hagan, *Chem. Commun.* **2010**, *46*, 139 – 141.

[14] M. Onega, M. Winkler, D. O'Hagan, *Future Med. Chem.* **2009**, *1*, 865 – 873.

[15] H. Deng, S. L. Cobb, A. R. McEwan, R. P. McGlinchey, J. H. Naismith, D. O'Hagan, D. A. Robinson, J. B. Spencer, *Angew. Chem. Int. Ed.* **2006**, *45*, 759 – 762; *Angew. Chem.* **2006**, *118*, 773 – 776.

[16] S. L. Cobb, H. Deng, A. R. McEwan, J. H. Naismith, D. O'Hagan, D. A. Robinson, *Org. Biomol. Chem.* **2006**, *4*, 1458 – 1460.

[17] M. Thomsen, S. B. Vogensen, J. Buchardt, M. D. Burkart, R. P. Clausen, *Org. Biomol. Chem.* **2013**, *11*, 7606 – 7610.

[18] M. E. Sergeev, F. Morgia, M. R. Javed, M. Doi, P. Y. Keng, *J. Mol. Catal. B* **2013**, *97*, 74 – 79.

[19] a) S. Thompson, Q. Zhang, M. Onega, S. McMahon, I. Fleming, S. Ashworth, J. H. Naismith, J. Passchier, D. O'Hagan, *Angew. Chem. Int. Ed.* **2014**, *53*, 8913 – 8918; *Angew. Chem.* **2014**, *126*, 9059 – 9064; b) S. Thompson, M. Onega, S. Ashworth, I. N. Fleming, J. Passchier, D. O'Hagan, *Chem. Commun.* **2015**, *51*, 13542 – 13545.

[20] S. Thompson, I. N. Fleming, D. O'Hagan, *Org. Biomol. Chem.* **2016**, *14*, 3120 – 3129.

[21] a) H. Tao, V. W. Cornish, *Curr. Opin. Chem. Biol.* **2002**, *6*, 858 – 864; b) C. A. Denard, H. Ren, H. Zhao, *Curr. Opin. Chem. Biol.* **2015**, *25*, 55 – 64; c) J. L. Porter, R. A. Rusli, D. L. Ollis, *ChemBioChem* **2016**, *17*, 197 – 203; d) P. Molina-Espeja, J. Vina-Gonzalez, B. J. Gomez-Fernandez, J. Martin-Diaz, E. Garcia-Ruiz, M. Alcalde, *Biotechnol. Adv.* **2016**, *34*, 754 – 767.

[22] a) U. T. Bornscheuer, M. Pohl, *Curr. Opin. Chem. Biol.* **2001**, *5*, 137 – 143; b) S. Lutz, *Curr. Opin. Biotechnol.* **2010**, *21*, 734 – 743; c) M. Kaushik, P. Sinha, P. Jaiswal, S. Mahendru, K. Roy, S. Kukreti, *J. Mol. Recognit.* **2016**, *29*, 499 – 503.

Received: July 21, 2016
Revised: August 24, 2016
Published online: ■■ ■■, ■■■■

Communications

Biocatalysis

H. Sun, W. L. Yeo, Y. H. Lim, X. Chew, D. J. Smith, B. Xue, K. P. Chan, R. C. Robinson, E. G. Robins, H. Zhao,* E. L. Ang* _____ ■■■■–■■■■

Directed Evolution of a Fluorinase for Improved Fluorination Efficiency with a Non-native Substrate

Faster Fluorination: Fluorinases are challenging to engineer owing to high substrate specificity. A fluorinase (structure shown) was engineered through directed evolution and the evolved variants showed improved activity with the non-native substrate 5′-chloro-5′-deoxyadenosine. Kinetics studies revealed a faster first step of the reaction. Structural data suggest that the mutations lead to tighter binding of *S*-adenosyl-L-methionine.